Numerical investigation of the role of topological defects in the three-dimensional Heisenberg transition

Man-hot Lau
School of Physics and Astronomy, University of Minnesota, Minneapolis, Minnesota 55455

Chandan Dasgupta
School of Physics and Astronomy, University of Minnesota, Minneapolis, Minnesota 55455
*and Department of Physics, Indian Institute of Science, Bangalore 560 012, India**
(Received 20 July 1988)

The role of topological point defects (hedgehogs) in the phase transition of the classical Heisenberg model in three dimensions is investigated by using Monte Carlo simulations. Simulations of the behavior of the defects near the phase transition show that the number density of defects increases sharply and defect pairs with separations comparable to the sample size begin to appear as the temperature is increased through the transition temperature. In simulations in a restricted ensemble in which spin configurations containing defects are not allowed, the system appears to remain ordered at all temperatures. Simulations in which the spin-spin interaction is set equal to zero and the number density of defects is controlled by varying a "chemical potential" term indicate that the system is ordered if the number density of defect pairs is sufficiently small. These results show that topological defects play a crucial role in the three-dimensional Heisenberg transition in the sense that configurations containing defect pairs are necessary for the transition from the ferromagnetic to the paramagnetic phase to occur.

I. INTRODUCTION

During recent years, many interesting results have been obtained from applications of algebraic topology, or more specifically, homotopy theory in the study of defects in ordered systems.[1] By using homotopy theory, it has been possible to systematically classify[1] different kinds of topologically stable defects. These are what we call *topological defects*. Common examples of topological defects are vortices in superfluids and superconductors and dislocations and disclinations in crystals and liquid crystals. The role of topological defects in phase transitions from ordered to disordered states has been a subject of much recent interest.[2] Theories[3] based on the statistical mechanics of topological defects have been successfully developed for a large class of two-dimensional phase transitions,[4] including the superfluid transition in thin ^{4}He films, the superconducting transition in thin metallic films, and the melting transition in two dimensions. According to these theories, the phase transitions from the ordered to the disordered phase in these systems correspond to an unbinding of pairs of point defects carrying topological charges of opposite sign. Recently, it has been shown that the superfluid[5] and superconducting[6] transitions in three dimensions and the nematic–to–smectic-A transition[7] in liquid crystals can be understood in terms of the statistical mechanics of interacting defect lines and loops. Also, there have been many attempts[8] to describe the melting of a crystal in terms of the behavior of dislocation loops. Topologically stable defects are known to exist in many more physical systems beyond those we have listed above. Therefore, it is interesting to inquire about the role of topological defects in phase transitions of other systems. In this paper, we are specifically interested in this aspect of the magnetic phase transition in the ferromagnetic classical Heisenberg model in three dimensions. The importance of a study of this model is attributed to the fact that this model is perhaps the most widely used one in describing the behavior of magnetic systems. The topological defects in the three-dimensional (3D) Heisenberg model are point singularities (the so-called "hedgehogs"). Their existence is a consequence of the nontrivialness of the second homotopy group $\pi_2(S_2)$.[1] These point defects carry integer-valued topological charges of both positive and negative sign. For example, a singularity of charge $+1$ occurs at a point if all the spins around it are directed radially outward from it. The energies associated with a single defect and with a pair of defects with equal but opposite charge have been calculated.[9,10] It is known[10] that the energy of a pair of oppositely charged defects increases linearly with the distance of separation.

In order to understand the role of topological defects in a phase transition, the following questions[2] should be addressed. (i) Are topological defects necessary for the phase transition? In other words, if we have a system in which topological defects are not allowed to occur, would the system still exhibit the same phase transition as the one found in the system with topological defects? If it is found that the elimination of the defects changes the nature of the transition or eliminates it altogether, then the conclusion would be that the defects are necessary for a correct description of the phase transition. (ii) Are topological defects sufficient to describe the transition? That is to say, is it possible to formulate a correct and complete description of the phase transition entirely in terms

of the statistical mechanics of a system of defects? Answers to these questions are known for several systems. For example, the Kosterlitz-Thouless theory[3] of the phase transition in the two-dimensional XY model shows that topological defects (vortices) are both necessary and sufficient for a complete description of this transition. However, no clear answers to these questions are available at present for the 3D Heisenberg model. This model has been studied extensively by using series expansion,[11] numerical simulations[12] and renormalization-group (RG) methods,[13] but no information is available at present about the behavior of the defects near the phase transition. In particular, it is not known whether the defect pairs unbind at the transition. The statistical mechanics of a system of point defects occurring in this model has not been worked out. A theoretical analysis of the role of defects in this system is made complicated by several factors. Since the nonsingular, spin-wave-type excitations in this model are nonlinear, it is not clear whether these excitations alone are sufficient to destroy long-range order in this model at a finite temperature. [In contrast, it is known that spin waves alone cannot destroy the (quasi-long-range) long-range order in the (two-) three-dimensional XY model.] In fact, renormalization-group calculations[14] near two dimensions on the O(n) nonlinear σ model, which presumably includes only long-wavelength spin-wave-like excitations, suggest that there is a finite-temperature phase transition at $n=d=3$ (d is the dimension of space). This result implies that spin waves in the 3D Heisenberg model may be sufficient to cause a transition to the disordered phase. Due to nonlinearities arising from the three-dimensional nature of the Heisenberg spins, the energy of an ensemble of point defects in the 3D Heisenberg model cannot be decomposed into a sum of pairwise terms. This further complicates any analysis of the statistical mechanics of the defect system. Furthermore, the decoupling between spin-wave and topological excitations found in XY-like models does not occur in the Heisenberg model. For these reasons, topological defects in the 3D Heisenberg model have not received a great deal of theoretical attention. We note that questions about the role of the defects in the phase transition of the continuum version of this model are closely related to the importance of allowing fluctuations in the magnitude of the ordering field[15] because such fluctuations are essential for the occurrence of singular defects. (The magnitude of the ordering field vanishes at the center of a defect).

There exists some speculation on the role of defects in the 3D Heisenberg phase transition. Several years ago, Cardy and Hamber[16] discussed the critical behavior of the O(n) model in d spatial dimensions in the neighborhood of $n=d=2$, assuming analyticity of the RG equations in n and d. Their analysis suggests that there exists a line $d=d_c(n)$ in the n-d plane which passes through the point $(n,d)=(2,2)$, and has the following property: for $n>2$, $d>2$, topological defects play a crucial role in determining the nature of the phase transition if $d \gtrsim d_c(n)$, and are unimportant if $d<d_c(n)$. Their analysis predicts the slope of the line $d=d_c(n)$ near $(n,d)=(2,2)$ to be $4/\pi^2$. This prediction implies that the point representing the 3D Heisenberg model in the n-d plane ($n=d=3$) lies in the region where topological defects are important, and suggests that the defects must be explicitly taken into account for a correct description of the critical behavior of the 3D Heisenberg model. We have recently performed a real-space renormalization group calculation[17] on the O(n) model for $1<n<2$ and $1<d<2$. Our calculated result on the slope ($\simeq 0.2$) of the line $d=d_c(n)$ near $n=2$ appears to be smaller than $4/\pi^2$, but nevertheless supports the conclusion reached by Cardy and Hamber on the importance of defects in the $n=d=3$ case. Qualitative arguments presented by Halperin[2] also suggest that defects are essential for the ferromagnetic to paramagnetic transition to occur in the continuum version of the 3D Heisenberg model. He pointed out the possibility that spin waves are probably not sufficient to destroy the long-range order in this model. These arguments, if correct, would have important implications on the present theoretical understanding of the 3D Heisenberg phase transition. In particular, both Cardy and Hamber[16] and Halperin[2] argue that singular defects are not properly taken into account in the RG calculations on the O(3) nonlinear σ model,[14] and therefore, these calculations do not describe the 3D Heisenberg transition correctly. It is interesting to note in this context that the values of the critical exponents for the $n=d=3$ transition obtained from an extrapolation of the ϵ-expansion ($\epsilon=d-2$) results[14] for the O(3) nonlinear σ model do not agree well with the currently accepted values obtained from series expansion[11] and RG (ϵ expansion where $\epsilon=4-d$) methods.[13]

Recently, the O(3) model and the associated topological excitations have received some attention in theoretical studies of high-temperature superconductivity. The O(3) nonlinear σ model has been used in a calculation[18] of the magnetic properties of high-T_c superconductors. Mechanisms involving topological defects have been proposed[19,20] as explanations of high-T_c superconductivity. We also note that an understanding of the behavior of defects in the 3D Heisenberg model would be relevant to a class of gauge field theories in which point singularities of a similar nature (e.g., monopoles) are known to occur.[21]

In this paper we present the results of a numerical investigation, using Monte Carlo (MC) simulations, of some of the questions mentioned above. A summary of the main results of this study was published earlier[22] in a letter. We first carried out a detailed MC simulation of the 3D Heisenberg model on a simple cubic lattice with special attention to the behavior of the defects. Using a definition of the topological charge appropriate for a lattice model, we calculated the temperature dependence of the number density ($\langle n \rangle$) of defects in the vicinity of the transition. We also calculated the usual thermodynamic quantities (energy, specific heat, magnetization, etc.) and used finite-size scaling to analyze the data. The values of the transition temperature and the critical exponents obtained from our calculations are in good agreement with the currently accepted results. Concerning the behavior of the topological defects, we found that $\langle n \rangle$ increases sharply as the temperature is increased through the transition temperature T_c. The temperature derivative

$d\langle n\rangle/dT$ exhibits a sharp peak at T_c. The temperature and sample-size dependence of $d\langle n\rangle/dT$ near $T=T_c$ is consistent with a divergence of this quantity with an exponent $\simeq 0.65$ at $T=T_c$. Defects with opposite charges are closely bound in pairs at low temperatures. As T approaches T_c from below, defects pairs with separations comparable to the lattice size begin to appear, suggesting an unbinding of defect pairs at T_c. The observed proliferation and unbinding of defect pairs at the transition are very similar to the behavior found in numerical simulations of 2D (Ref. 23) and 3D (Ref. 5) XY transitions which are known to be mediated by topological defects. Our results, therefore, suggest that the defects probably play an important role in the 3D Heisenberg transition also.

In order to determine whether the defects are indeed necessary for this transition, we next carried out a MC simulation in which spin configurations containing defects are not allowed to occur. This was done by starting with a spin configuration that contains no defect, and then using a MC updating procedure that rejects any "move" that would create a defect pair. We did not find any evidence for a phase transition in these simulations. All thermodynamic functions were found to vary smoothly with temperature at all temperatures up to $T\rightarrow\infty$, and the magnetization appeared to remain finite in the $T\rightarrow\infty$ limit. These results indicate that configurations containing topological defects are necessary for the transition to the disordered phase to occur. We also carried out a simulation in which the strength of the nearest-neighbor spin-spin interaction was set equal to zero, and a "chemical potential" term determining the number density of defects was varied. We found strong evidence indicating that the system remains ordered at all temperatures if the number density of defects is sufficiently small, in agreement with the previous conclusion that the defects are necessary for the 3D Heisenberg transition. This is the main result of our calculation. All the results described above are qualitatively very similar to those found in a recent MC study[5] of the role of vortex loops in the 3D XY transition.

We organize the rest of the paper as follows: Section II contains a description of the models studied in this work and the procedures used in the numerical simulations. The results obtained from the simulations are described in detail in Sec. III. Section IV contains a discussion of some of the questions raised by our calculations.

II. THE MODELS AND SIMULATION PROCEDURES

The classical Heisenberg model considered in this paper is defined on a 3D simple cubic lattice by the reduced Hamiltonian

$$H=-K\sum_{\langle ij\rangle}\mathbf{S}_i\cdot\mathbf{S}_j\ , \tag{2.1}$$

where $\mathbf{S}_i$'s are three-dimensional vectors of unit length located at the lattice sites, $\langle ij\rangle$ represents distinct nearest-neighbor pairs of lattice sites, and $K=J/k_BT$, $J>0$. We set $J=k_B=1$, so that $K=1/T$ in our notation. This model shows a second-order phase transition from the ordered ferromagnetic phase to the disordered paramagnetic phase at $T\simeq 1.45$.[11,12] The topological charge Q of a point defect in this model represents the number of times and the sense in which spins on a closed surface surrounding the defect cover the surface of a unit sphere in spin space. In the continuum limit, the topological charge Q enclosed by a closed surface Ω in real space is defined[1] through an integration of the Jacobian of the spin-space variables Θ,Φ (these are the angles specifying the orientation of the spin field $\mathbf{S}$) over the surface Ω:

$$Q=\frac{1}{4\pi}\int J(\Theta(x,y),\Phi(x,y))d\Omega(x,y)\ , \tag{2.2}$$

where x,y are generalized coordinates on the surface Ω. For the lattice model (2.1), we need a different definition of Q. In this work, we have defined Q by using a prescription similar to one used by Berg and Lüscher[24] to classify instanton configurations in the 2D Heisenberg model on a lattice. This is done in the following way: For each unit cube of the lattice, we divide the six faces into 12 triangles, two for each face. Let $\mathbf{S}_1(i)$, $\mathbf{S}_2(i)$, and $\mathbf{S}_3(i)$ be the three spins at the corners of the triangle i where the sequence 1,2,3 is chosen such that the circuit $1\rightarrow 2\rightarrow 3\rightarrow 1$ corresponds to a counterclockwise rotation along the outward normal to the surface of the triangle. We then calculate the area, $\Delta(i)$, of the spherical triangle formed by the three spins on the surface of a unit sphere. This area $\Delta(i)$ is also given a sign which is $\mathrm{sgn}\{\mathbf{S}_1(i)\cdot[\mathbf{S}_2(i)\times\mathbf{S}_3(i)]\}$. The topological charge Q enclosed by the unit cube is then given by

$$Q=\sum_{i=1}^{12}\Delta(i)\ . \tag{2.3}$$

This procedure corresponds to an interpolation of the spin field along geodesic lines on a unit sphere in spin space. Apart from a set of "exceptional" configurations[24] of measure zero, this prescription yields well-defined integral values for Q. Moreover, this definition of Q ensures that the net topological charge is always equal to zero in a system with periodic boundary conditions.

The standard Metropolis algorithm[25] was used in the MC simulations. In this algorithm, a MC update of a spin consists of the following steps: First, the angle associated with an attempted change of a spin is chosen at random from within a specified range. Then the energy change, ΔE, associated with the attempted update is calculated. If $\Delta E\leq 0$, the change is accepted. If $\Delta E>0$, the change is accepted with a probability $\exp(-\Delta E/T)$. These simulations were performed on the CRAY 2 Computer at the Minnesota Supercomputer Institute. To take advantage of the vectorizing capability of the CRAY, we divided our 3D lattice into four sublattices in such a way that the calculation of ΔE for the updating of a spin on a particular sublattice does not involve any other spin belonging to the same sublattice. All spins belonging to one of the four sublattices could then be updated simultaneously in a single vectorized step. In our study of the equilibrium behavior of the defects near the phase transition, we carried out simulations for samples with linear dimension $L=8$, 12, and 16 using periodic boundary conditions. Standard methods were used in the calculations of

equilibrium averages. Typically, 1000–2000 MC steps per spin were used for equilibration and 4000–8000 steps per spin were used for calculating averages.

We also carried out MC simulations with a modified reduced Hamiltonian

$$H' = -K \sum_{\langle ij \rangle} \mathbf{S}_i \cdot \mathbf{S}_j + \lambda \sum_{\text{cubes}} |Q| \ , \tag{2.4}$$

where the new terms acts as a "chemical potential" for the defects. For $\lambda > 0$, this term has the effect of suppressing configurations containing defects. In simulations with this reduced Hamiltonian, a calculation of ΔE, the energy change associated with an attempted update of a spin, involves calculations of the changes in the topological charges associated with the eight unit cubes which share the spin under consideration. These calculations require a large amount of computation. Because of this reason, and the fact that the vectorization procedure described earlier does not work for the reduced Hamiltonian (2.4), our simulations with this reduced Hamiltonian were restricted to relatively small samples ($L \leq 10$).

The $\lambda \rightarrow \infty$ limit of (2.4) corresponds to an ensemble in which configurations containing topological defects are not allowed. Simulations in that restricted ensemble were performed by using the following MC updating procedure. We started with a configuration (e.g., the fully aligned ferromagnetic ground state) in which there are no defects. Each update attempt was then checked to determine whether it would create a defect pair. If it did, then the attempted change was rejected; otherwise, it was accepted or rejected according to the usual Metropolis algorithm described earlier in this section. Simulations in the ensemble without defects were performed for samples with $L = 6$, 8, and 12.

III. RESULTS

In this section, we describe in detail the results obtained from our MC simulations.

A. Thermodynamic properties

In our simulations of the model defined by the reduced Hamiltonian (2.3), we calculated the usual thermodynamic functions as a test of the simulation procedure. The results for the internal energy per spin ($\langle E \rangle$, where $\langle \cdots \rangle$ denotes a MC average) and the specific heat (C) are shown in Figs. 1 and 2, respectively. The specific-heat data shown in Fig. 2 were obtained from a numerical differentiation of the internal energy $\langle E \rangle$ with respect to the temperature T. The specific heat peaks at approximately the same temperature for three different values of L. The specific-heat peak becomes sharper as L is increased, as expected for a continuous phase transition. We also calculated the average of M, the magnitude of the magnetization,

$$M = \left| \frac{1}{N} \sum_i \mathbf{S}_i \right| \ , \tag{3.1}$$

where $N = L^3$ is the total number of spins. Since the MC updating procedure generates uniform rotations of the spin system, a calculation of the MC average of $\mathbf{M}$ is not meaningful. The results for the temperature dependence of $\langle M \rangle$ are shown in Fig. 3. As expected, we find a sharp change in $\langle M \rangle$ at a temperature close to that of the specific-heat peak ($T \simeq 1.45$). We used standard finite-size scaling analysis[26] to extract the values of the transition temperature and the critical exponents from the MC data. A finite-size scaling plot for $\langle M \rangle$ is shown in Fig. 4. Near $T = T_c$, the temperature and sample-size dependence of $\langle M \rangle$ is expected to be of the form

$$\langle M(L,T) \rangle = L^{-\beta/\nu} g_1(tL^{1/\nu}) \ , \tag{3.2}$$

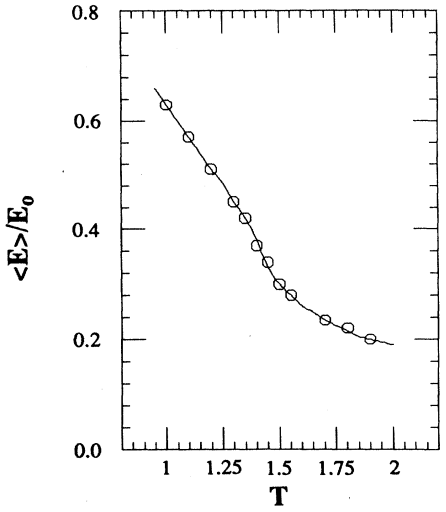

FIG. 1. The internal energy per spin $\langle E \rangle$ vs temperature T for $L = 16$. $E_0 = -3$ is the ground-state energy per spin. The solid line is a guide to the eye.

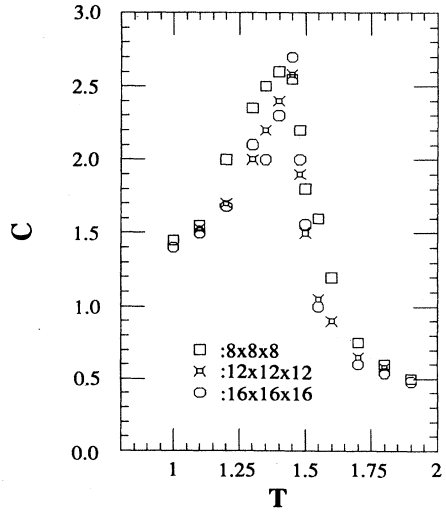

FIG. 2. Temperature dependence of the specific heat C for three different samples sizes.

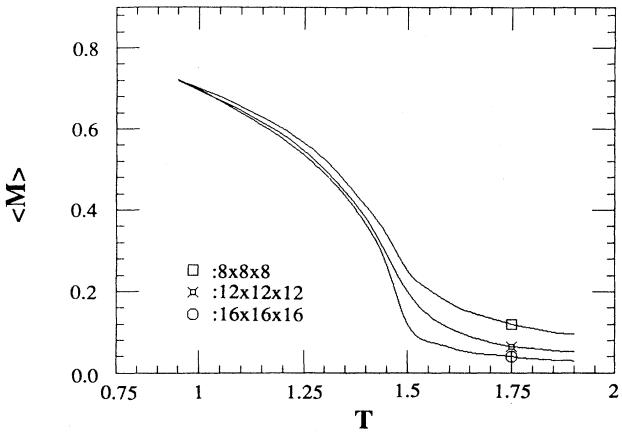

FIG. 3. Temperature dependence of $\langle M \rangle$, the magnetization per spin, for three different sample sizes. The solid curves are lines drawn through the data points.

where $t=(T-T_c)/T_c$ and β, ν are the critical exponents for the magnetization and the correlation length, respectively. As shown, in Fig. 4, plots of $\langle M \rangle L^{\beta/\nu}$ versus $tL^{1/\nu}$ for different L fall on the same scaling curve for a proper choice of the values of T_c, β, and ν. Similar scaling fits were also obtained for the specific-heat data. The results obtained from the finite-size scaling analysis are

$$T_c=1.45\pm0.02, \quad \nu=0.705\pm0.005 ,$$
$$\beta=0.36\pm0.04, \quad \alpha=-0.11\pm0.06 .$$

These values are in good agreement with the currently accepted results[11–13] for the 3D Heisenberg transition.

In the simulations, we also calculated the averages of M^2 and M^4. The ratios, $\langle M^2 \rangle / \langle M \rangle^2$ and $\langle M^4 \rangle / \langle M^2 \rangle^2$ are expected to have particularly simple finite-size scaling forms, and these ratios of moments of the order parameter distribution function have proven to be very useful[27] in the analysis of numerical data on systems exhibiting continuous phase transitions. From standard finite-size scaling arguments, we have, near $T=T_c$,

$$\langle M^2(L,T) \rangle = L^{-2\beta/\nu} g_2(tL^{1/\nu}) ,$$
$$\langle M^4(L,T) \rangle = L^{-4\beta/\nu} g_3(tL^{1/\nu}) . \tag{3.3}$$

Combining these with (3.2), we have

$$R_1(L,T) \equiv \langle M^2(L,T) \rangle / \langle M(L,T) \rangle^2 = G_1(tL^{1/\nu}) ,$$
$$R_2(L,T) \equiv \langle M^4(L,T) \rangle / \langle M^2(L,T) \rangle^2 = G_2(tL^{1/\nu}) . \tag{3.4}$$

These equations tell us that plots of R_1 or R_2 versus T for different sample sizes should intersect one another at $T=T_c$. Such a crossing of the R_1 (or R_2) versus T curves for different L has been used in several recent studies[27,28] as a criterion to determine whether a phase transition takes place or not. Our results for R_1 and R_2 are somewhat noisy. Nevertheless, the data unambiguously exhibit a crossing of the R_1, R_2 versus T curves in the neighborhood of $T=T_c$, with R_1, R_2 increasing with L at temperatures higher than T_c, and decreasing with L at temperatures lower than T_c. Another interesting feature we find is that even for temperatures slightly below T_c, both R_1 and R_2 are very close to unity ($R_1<1.03$ and $R_2<1.1$ for $T\leq1.4$) and their L dependence is very weak. This feature may be a reflection of the fact that both transverse and longitudinal correlation lengths are infinite at all temperatures below T_c in the isotropic Heisenberg model. These features in the observed L dependence of R_1 and R_2 will be useful later when we address the question of whether a phase transition takes place when topological defects are suppressed.

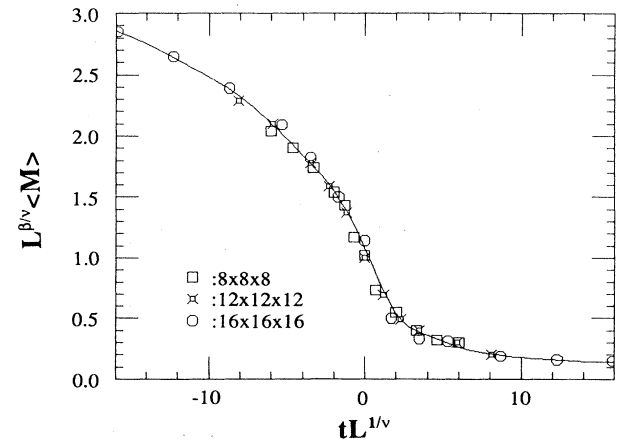

FIG. 4. Finite-size scaling plot ($T_c=1.45$, $\nu=0.705$, $\beta=0.36$) for $\langle M \rangle$ [see Eq. (3.2)]. The solid line is a guide to the eye.

B. Behavior of topological defects near T_c

At regular intervals along the MC evolution of the system at a fixed temperature near T_c, we examined the spin configurations and used the prescription outlined in Sec. II to determine the topological charge Q associated with each unit cube of the sample. We found that the magnitude of the nonzero charges is almost always equal to unity. Only a few defects with $Q=\pm2$, and none with $|Q|>2$ were found. The temperature dependence of the average defect pair density $\langle n \rangle$ ($n=$ number of defect pairs divided by N) is shown in Fig. 5. The density of defects is found to increase sharply as T increases through T_c. The rapid increase of $\langle n \rangle$ near T_c can be seen more clearly in the inset of Fig. 5 where we show the temperature dependence of the numerically calculated derivative $d\langle n \rangle/dT$ for two different sample sizes. The temperature at which $d\langle n \rangle/dT$ peaks is identical within error bars to the T_c determined from thermodynamic data. The peak of $d\langle n \rangle/dT$ becomes sharper and increases in height as L increases, suggesting that $d\langle n \rangle/dT$ diverges at $T=T_c$ in the thermodynamic limit. Assuming that

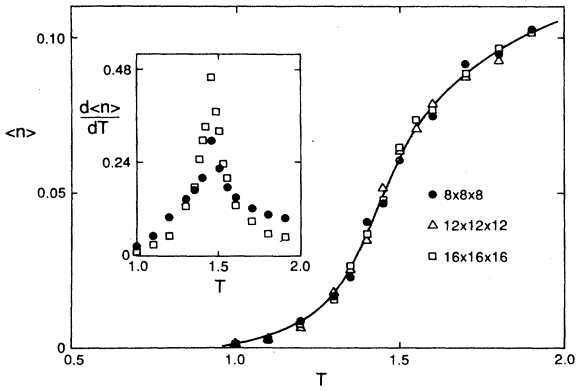

FIG. 5. Temperature dependence of $\langle n \rangle$, the average number density of defect pairs. The solid curve is a guide to the eye. The inset shows plots of $d\langle n \rangle/dT$ vs T for two different sample sizes (squares, $L=16$; solid circles, $L=8$).

$d\langle n \rangle/dT$ diverges at T_c with an exponent ψ, we have the following finite-size scaling form for $d\langle n \rangle/dT$ near $T=T_c$:

$$\frac{d\langle n(L,T)\rangle}{dT} = L^{\psi/\nu} f(tL^{1/\nu}) . \tag{3.5}$$

As shown in Fig. 6, the data for $d\langle n \rangle/dT$ are consistent with this scaling form with $\psi \simeq 0.65$ and the previously determined values for T_c and ν. It is interesting to note that $\psi = 1-\beta$ within error bars. This result suggests that the defect pair density $\langle n \rangle$ perhaps plays the role of a "disorder variable" whose critical behavior is described by the same exponent (β) as that for the order parameter $\langle M \rangle$. We, however, do not have other evidence supporting this interpretation and the apparent equality of ψ and $(1-\beta)$ may be just a coincidence.

At low temperatures, the defect pair density is expected to be proportional to $\exp(-E_0/T)$ where E_0 is the minimum energy required to create a pair of oppositely charged defects. As shown in Fig. 7 where we have plotted $\ln\langle n \rangle$ versus $1/T$, our results for $\langle n \rangle$ at temperatures below T_c are well described by the expected activated form. Deviations from this form are observed as T approaches T_c from below. The value of E_0 obtained from a straight line fit to the $\ln\langle n \rangle$ versus $1/T$ plot for $T < T_c$ is $E_0 = 12.7 \pm 0.7$. This value is close to 4π, the value expected[10] for the energy of a defect pair separated by unit distance in the continuum limit.

An important question is whether the observed proliferation of defects as T increases through T_c is accompanied by an unbinding of defect pairs. We investigated this aspect of the phase transition by carefully examining the defect configurations generated in the MC simulations at different temperatures close to T_c. At low temperatures, we find that defects with opposite charges are closely bound together, the separation being just one lattice spacing for most pairs. As T approaches T_c from below, the number of defects increases sharply and it becomes difficult to pair up defects with opposite charges in an unambiguous way. A reasonable choice for the pairing up of defects with opposite charges would be to take the pairing that minimizes the total "string length," i.e., the sum of the pair separations. However, a determination of the pairing that globally minimizes the total string length for a system with a large number of defects is a difficult optimization problem (the so-called "matching problem"[29] in the literature on combinatorial optimization). We developed a heuristic algorithm for finding the optimal pairing and tested it on small samples for which

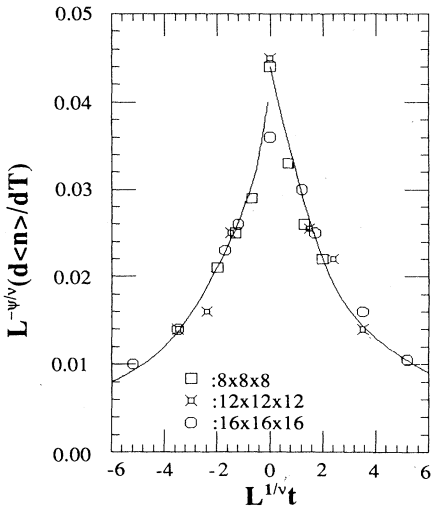

FIG. 6. Finite-size scaling plot for $d\langle n \rangle/dT$, assuming the scaling form given in Eq. (3.5). The values of the parameters are $T_c = 1.45$, $\nu = 0.705$, and $\psi = 0.65$. Solid lines are guides to the eye.

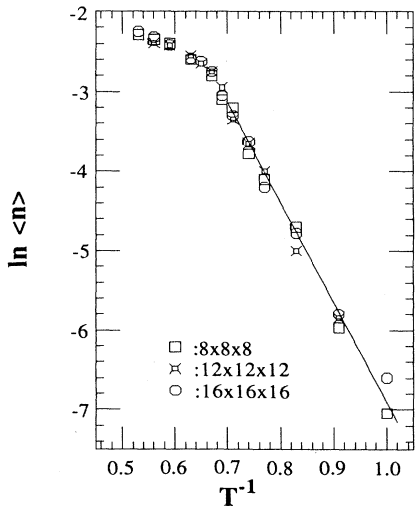

FIG. 7. Plot of the natural logarithm of the defect-pair density vs the inverse temperature. The solid line is a linear fit to the data for $T < T_c$.

the optimal pairing could be determined by inspection. The algorithm was found to select the correct pairing in all the test cases. However, we are not sure about whether this algorithm always finds the globally optimal pairing in large samples, although we are confident that it selects a near optimal pairing in all cases. We used the pairings selected by this algorithm to compute the distribution of pair separations. We found that pairs with separations comparable to $L/2$ appear at temperatures close to or above T_c. (Note that the largest separation possible in a $L\times L\times L$ sample with periodic boundary condition is $\sqrt{3}L/2$.) In Fig. 8, we have shown the distribution of pair separations for the $L=16$ sample at two temperatures, $T=1.3$ and $T=1.6$. At $T=1.3$, which corresponds to being in the ordered phase, all defect pairs have separations less than 2.5 units. In contrast, at $T=1.6$, which is somewhat higher than T_c, the distribution of pair separations extends up to nine units. It is difficult to draw any quantitative conclusion about the unbinding of the defect pairs from the data on the distribution of pair separation. In particular, it is not possible to pinpoint a temperature at which the defect pairs unbind. Nevertheless, the observed behavior is certainly consistent with an unbinding of defect pairs at the transition temperature.

All the features described above in the behavior of the defects near the phase transition are qualitatively very similar to those found in simulations of 2D (Ref. 23) and 3D (Ref. 5) XY transition which are known to be mediated by defects. These results, therefore, suggest that topological defects play an important role in the 3D Heisenberg transition also.

C. Simulations in a restricted ensemble with no defects

In order to determine whether topological defects are indeed necessary for the 3D Heisenberg transition, we carried out a set of MC simulations with the reduced Hamiltonian (2.4) which contains a new term that acts as a chemical potential for the defects. We first considered the limit $\lambda\rightarrow\infty$ which corresponds to restricting the ensemble to configurations containing no defects. The MC procedure used in the calculation of averages in this restricted ensemble is described in Sec. II. In these simulations, we did not find *any* evidence for a phase transition from the ordered to the disordered phase at *any* temperature. The thermodynamic quantities $\langle E\rangle$, C, and $\langle M\rangle$ were found to change smoothly with temperature at all temperatures up to $T\rightarrow\infty$ ($K=0$). The specific-heat data for $L=12$ are shown in Fig. 9 where we have also shown the results for the original model (2.1) for comparison. For temperatures $T<1.0$, the specific heat data obtained from simulations without defects are essentially identical to those obtained from the unrestricted simulations. This is not surprising because, as can be seen in Fig. 5, the defect pair density calculated in the unrestricted ensemble is vanishingly small at temperatures lower than $T=1.0$. At higher temperatures, however, we find a big difference. In particular, the specific-heat peak that signals the phase transition in the original model disappears completely when defects are not allowed. The results for $\langle M\rangle$ obtained from the restricted simulations are shown in Fig. 10. We find that the magnetization remains nonzero at all temperatures. The average value of M defined in (3.1) is, of course, always nonzero for a finite-size system. However, $\langle M\rangle$ is expected to be proportional to $1/\sqrt{N}$ if the system does not have long-range order. In the inset of Fig. 10, we have plotted values of $\langle M\rangle$ at $K=0$ ($T\rightarrow\infty$) versus $1/\sqrt{N}$. Clearly, there is no indication of $\langle M\rangle$ extrapolating to zero in the $N\rightarrow\infty$ limit. The sample-size dependence of $\langle M\rangle$ is, in fact, well described by the form $\langle M\rangle=M_0+a/\sqrt{N}$ with $M_0\simeq 0.18$ and $a\simeq 1.2$. This observation indicates that

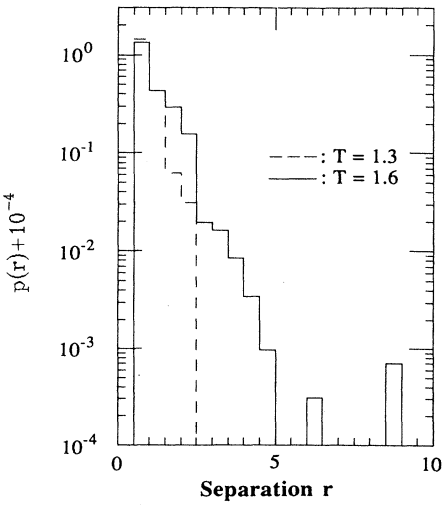

FIG. 8. The distribution of the separation r between two oppositely charged defects belonging to a pair at two temperatures (solid line, $T=1.6$; dashed line, $T=1.3$) for $L=16$. Here, $p(r)\Delta r$ with $\Delta r=0.5$ is the probability of having a defect pair with separation between $r-\Delta r$ and r.

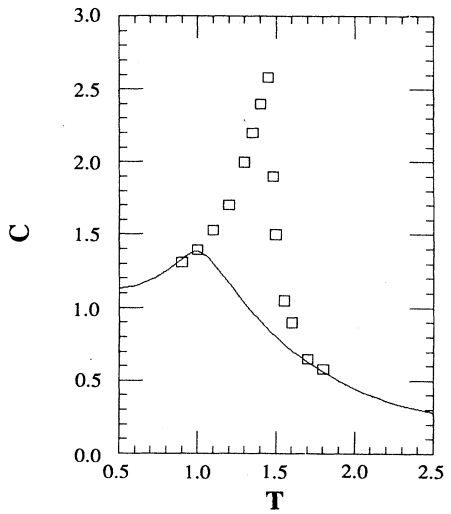

FIG. 9. Temperature dependence of the specific heat for $L=12$ (solid line) when defects are not allowed. The results for $L=12$ obtained from the unrestricted simulation are also shown (squares) for comparison.

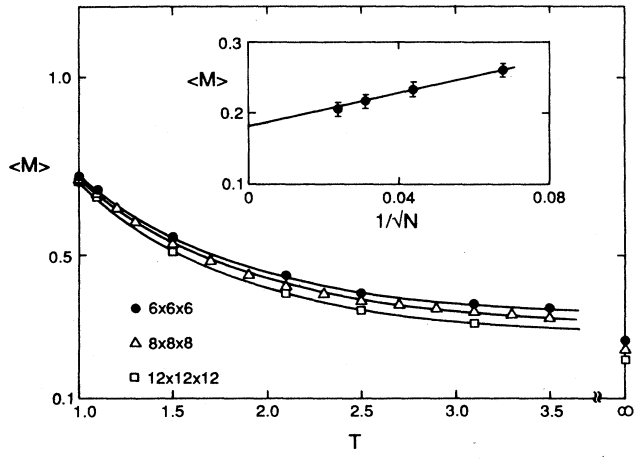

FIG. 10. Temperature dependence of the magnetization $\langle M \rangle$ obtained from simulations in which defects are not allowed. Solid curves are guides to the eye. The inset shows a plot of $\langle M \rangle$ at $T \to \infty$ vs $1/\sqrt{N}$, N being the number of spins. The straight line is the best linear fit to the data.

the nonvanishing of $\langle M \rangle$ found in the restricted simulation is not a trivial finite-size effect. In the spin-wave approximation, the two-point correlation function in the ordered phase is expected to have the form

$$\langle \mathbf{S}(0) \cdot \mathbf{S}(\mathbf{r}) \rangle \sim M_0^2 + b/r \tag{3.6}$$

at long distances, where M_0 is the spontaneous magnetization. This translates into the following dependence of $\langle M \rangle$ on the sample size N:

$$\langle M \rangle = M_0 + A/N^{1/3} . \tag{3.7}$$

Our data for $\langle M \rangle$ at $K=0$ are consistent with this form with $M_0 \simeq 0.15$ and $A \simeq 0.65$, indicating a state with long-range order at all temperatures.[30] We also studied the temperature and sample-size dependence of the ratios of moments, R_1 and R_2, defined in (3.4). We found that both R_1 and R_2 remain close to unity ($R_1 < 1.02, R_2 < 1.08$) at all temperatures up to $T \to \infty$. Also, values of R_1 and R_2 decrease with increasing L at all temperatures, and there is no sign of any crossing of the R_1, R_2 versus T curves for different L. As discussed in Sec. III B, the ratios R_1 and R_2 were found to exhibit very similar behavior in the ordered phase of the original model. All these results consistently indicate that the system remains ordered at all temperatures if configurations containing defects are not allowed.

There is one question that needs to be resolved before we can consider the results described above as conclusive evidence indicating that the defects are necessary for the phase transition. Since most of the data in the $\lambda \to \infty$ limit were obtained from simulations in which the system was warmed up from the ground state, we have to consider the possibility that the observed behavior is caused by a trapping of the system in a small region of phase space with nonzero M and is, therefore, an artifact of the MC procedure used by us. The standard MC method is guaranteed to generate the appropriate ensemble averages if any two points in the allowed phase space are connected by a path with a nonzero transition probability. Since a class of configurations (those with topological defects) are assigned zero probability in the $\lambda \to \infty$ limit, it is not clear *a priori* whether this connectedness criterion is satisfied or not. To investigate this question, we repeated the simulations at $K=0$ with two other starting configurations with no defects, one with $M=0$ and the other with $M=0.5$. As shown in Fig. 11, all these runs converge to the same value, $\langle M \rangle \simeq 0.23$ within ~ 1000 MC steps/spin, thus indicating that the parts of phase space with $M=0$ are indeed connected to those with nonzero values of M. This observation confirms that the observed nonvanishing of $\langle M \rangle$ is not caused by a trapping of the system in phase space.

D. Simulations with a chemical potential for defects

We have also simulated the behavior of the model Hamiltonian (2.4) as a function of λ with $K=0$. Questions about the phase space breaking up into disconnected regions do not arise in these simulations as long as the value of λ is not very large. The variation of $\langle M \rangle$ with λ obtained from these simulations is shown in Fig. 12. We find a rapid change of $\langle M \rangle$ near $\lambda = \lambda_c \simeq 2$. As shown in Fig. 13, the N dependence of $\langle M \rangle$ is well described by the form $\langle M \rangle \propto 1/\sqrt{N}$, which is characteristic of the disordered phase, if λ is appreciably smaller than λ_c. For values of λ somewhat larger than λ_c, the variation of $\langle M \rangle$ with N is similar to that shown in the inset of Fig.

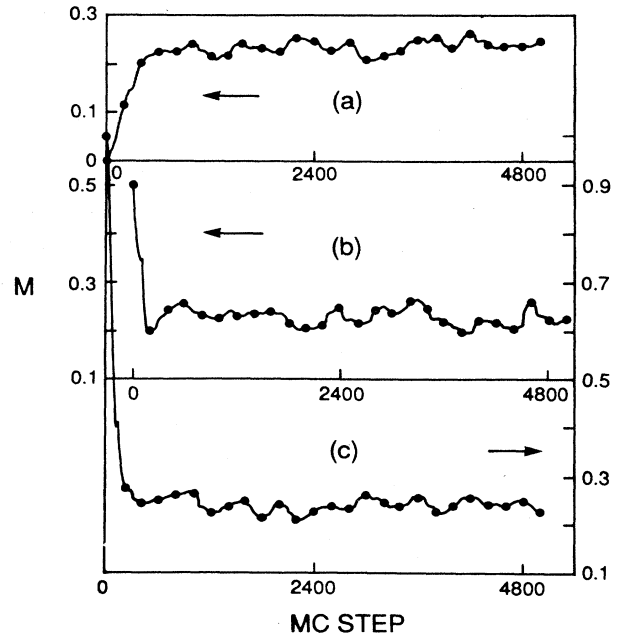

FIG. 11. Evolution of the magnetization M in MC simulations ($L=8$, $T \to \infty$) with no defects for three different starting configurations: (a) $M=0$, (b) $M=0.5$, and (c) $M=1.0$.

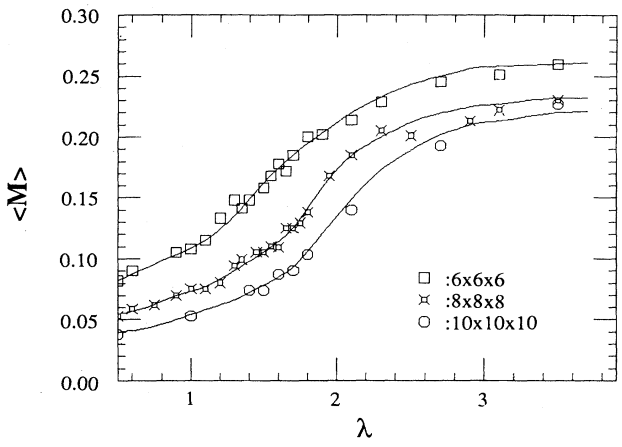

FIG. 12. Dependence of the magnetization $\langle M \rangle$ on the parameter λ [see Eq. (2.4)] at $K=0$. Solid lines are guides to the eye.

10, suggesting a state with long-range ferromagnetic order. For values of λ close to λ_c, the N dependence of $\langle M \rangle$ does not fit the form $\langle M \rangle = M_0 + aN^{-1/2}$. This presumably indicates critical behavior. These observations suggest a transition from the disordered to the ordered phase as λ is increased through λ_c. The behavior of the ratios of moments, R_1 and R_2, is consistent with this picture. These results, thus, indicate that the system remains ordered at all temperatures if λ is sufficiently large, in agreement with the conclusion drawn in Sec. III C from the simulations in the $\lambda \to \infty$ limit. Due to the smallness of the sizes of the samples simulated with the reduced Hamiltonian (2.4), we could not obtain accurate

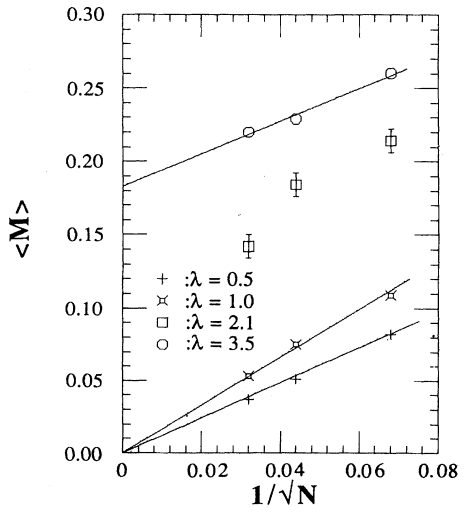

FIG. 13. Plots of the magnetization $\langle M \rangle$ at $K=0$ vs $1/\sqrt{N}$ for four different values of λ. The error bars are smaller than the sizes of the symbols except for $\lambda = 2.1$.

estimates of the critical value, λ_c, of λ and the values of the critical exponents describing the transition at $\lambda = \lambda_c$.

IV. DISCUSSION

The main result of the numerical study reported in this paper is the demonstration that point defects (hedgehogs) play a crucial role in the phase transition of the classical Heisenberg model in three dimensions. The number of defect pairs increases dramatically and the distribution of pair separation extends up to distances comparable to the lattice size as the transition temperature is approached from below. These observations suggest that the phase transition from the ferromagnetic to the paramagnetic state is accompanied by an unbinding of defect pairs. Simulations in which configurations containing defects are sufficiently suppressed or eliminated completely do not show any evidence for a transition to the paramagnetic phase, thus indicating that the point defects are indeed necessary for the phase transition. These results raise several interesting questions relating to the nature of the 3D Heisenberg transition. We conclude with a discussion on some of these questions.

As mentioned in the Introduction, questions about the importance of defects in the 3D Heisenberg transition are closely related to the validity of the O(n) nonlinear σ model in describing the phase transition in the $n=d=3$ model. In the nonlinear σ model, the spin field is assumed to have a fixed magnitude. If the model is defined on a continuum, and if one demands that the spin field varies smoothly and continuously (so that the derivatives $\nabla_\mu \mathbf{S}$ are well defined and finite) at all points in space, then it is not possible to have spin configurations containing singular point defects in this model. (At the center of such a point defect, the direction of the spin cannot be defined. Therefore, the magnitude of the spin field must vanish there.) One would then conclude that the O(3) σ model in three dimensions includes only nonsingular spin-wave-like excitations, and therefore, according to the results of our numerical calculations, this model does not exhibit any transition to the disordered phase. This conclusion would contradict the results of RG calculations[14] on the σ model, which indicate a finite-temperature phase transition in the $n=d=3$ model. This contradiction, however, is not a very serious one because the RG calculations are carried out in $(2+\epsilon)$ dimensions and an extrapolation of the results to three dimensions ($\epsilon=1$) is certainly open to questions. One may, however, adopt a different point of view about the nature of the nonlinear σ model. One may argue that the model in which the spin field is defined at every point in space (i.e., in which fluctuations of all length scales are allowed) is not well defined due to the presence of ultraviolet divergences. To get a well-defined field theory, it is necessary to adopt a regularization scheme. If the field theory is regularized by putting the spins on a lattice (which approximately corresponds to the usual introduction of an ultraviolet cutoff), then one ends up with a model that is identical to the lattice model studied here, which clearly includes both spin-wave and topological excitations. It is not clear to us whether other regulariza-

tion schemes lead to the same conclusion about the presence of defects in the 3D O(3) σ model. Nevertheless, a question that remains is whether the RG recursion relations obtained[14] for the O(n) σ model in $2+\epsilon$ dimensions properly take into account the topological excitations. There are reasons to believe that they do not describe correctly the contribution of the topological defects. This is clearly the situation for the XY model ($n=2$) at $d \geq 2$. The RG equations for the $n=2$ nonlinear σ model do not predict any transition to a disordered phase for any dimension $d \geq 2$, whereas we know that this model exhibits defect-mediated transitions from the ordered to the disordered phase in both two and three dimensions. In the XY model, there is a clear separation between spin-wave and topological excitations, and one can unambiguously associate the O(2) σ model with the spin waves which, being Gaussian, can not induce a transition to the disordered phase. Because of the nonlinearities inherent to the σ model with $n > 2$, a similar interpretation of the RG results for $n=3$ is much less certain. Our numerical results indicate that if the RG equations for the σ model do not include the effects of topological excitations, then they are not appropriate for a correct description of the $n=d=3$ transition.

Another interesting question concerns the nature of the phase diagram of the generalized Heisenberg model defined in (2.4). We have studied the behavior of this model along the lines $\lambda=0$ and $K=0$ in the (K-λ) plane and have found continuous phase transition at the points $(K_c,0)$ and $(0,\lambda_c)$. The transition at $(K_c,0)$ is the usual 3D Heisenberg transition, whereas the universality class of the transition at $(0,\lambda_c)$ is not known at the present time. We believe that there is a continuous phase boundary joining the points $(K_c,0)$ and $(0,\lambda_c)$ in the (K-λ) plane which separates the paramagnetic phase from the ferromagnetic one. We do not, however, have any information at the present time on the nature of critical behavior at points other than $(K_c,0)$ on this phase boundary. We wish to point out that our conclusion about the defects being necessary for the phase transition does not necessarily imply that the defect chemical potential λ is relevant (in the RG sense) at the critical point $(K_c,0)$. The fact that the system is ordered for all values of K if $\lambda > \lambda_c$ does not tell us anything about the nature of the phase transition for $0 < \lambda < \lambda_c$. Thus, our claim that the 3D Heisenberg transition is "mediated" by defects should not be interpreted as implying that λ is a relevant variable. In fact, there is some reason to believe that phase transitions for small but nonzero values of λ belong to the same universality class as the one for $\lambda=0$. If we assume that the phase transition is described correctly by the statistical mechanics of the system of defects (the plausibility of such a description is discussed later in this section), then we may argue that since the introduction of a small λ term changes only the short-distance part of the defect Hamiltonian, it should not affect the nature of the transition. The phase transition at the point $(0,\lambda_c)$ should, on the other hand, be unstable with respect to introducing the K term because this corresponds to turning on a long-range interaction between defects. Thus, it is plausible to expect a phase diagram in which all points other than $(0,\lambda_c)$ on the phase boundary belong to the 3D Heisenberg universality class, and the transition at $(0,\lambda_c)$ is of a different nature. A similar phase diagram was proposed and verified numerically[6] for a generalized version of the 3D XY model. Whether the same picture is valid for the 3D generalized Heisenberg model is unclear at present. Numerical investigations of this question would be very interesting.

Finally, we note that our conclusion that topological defects play a crucial role in the 3D Heisenberg transition introduces a completely new approach to a theoretical understanding of this transition. In particular, it raises the possibility of formulating a theory of the critical behavior at this transition in terms of the statistical mechanics of the system of point defects. Because of nonlinearities arising from the three-dimensional nature of the Heisenberg spins, a description of this transition in terms of defects would, however, be much more complicated than Kosterlitz-Thouless-type theories[3,4] of defect-mediated transitions in XY-like systems. Some of the difficulties encountered in such an approach were discussed in the Introduction. A necessary ingredient for a calculation of the statistical mechanics of the defect system is detailed information about how the energy of a defect ensemble depends on the positions and the topological charges of the defects. As discussed in the Introduction, the present knowledge on this question is incomplete. The energy associated with a single pair of oppositely charged defects has been calculated[10] for the continuum version of the model. It is not known whether this calculation is applicable without any modification to defects on a lattice. We are not aware of any calculation of the energy associated with more than one pair of defects. We have carried out a few preliminary numerical calculations bearing on these questions. In these calculations, we determined the energies associated with lowest-energy spin configurations containing a specified arrangement of point defects. The lowest-energy configurations were obtained by using a "zero-temperature" MC algorithm in which an attempted update of a spin is accepted only if it decreases the energy and it does not alter the specified arrangement of defects. We first considered the case where there are only two defects with $Q=\pm 1$, separated by a distance of d lattice spacings along one of the cubic axes. We found that the dependence of the energy E on the separation d is well approximated by the linear relation $E=Ad$ with $A \simeq 4\pi$, the value obtained[10] in the continuum limit. We also considered the situation where there are two defect pairs placed head to tail along a line parallel to one of the cubic axes. The two oppositely charged defects in each pair were separated by unit lattice spacing. We found that the total energy of this configuration of defects is well approximated by the sum of the two pair energies if the separation between the defect pairs is larger than ~ 4 lattice spacings. At smaller separations, we find a smaller value for the total energy and a simple superposition of pair potentials does not seem to work. This observation suggests that nonlinearities arising from the three-dimensional nature of the Heisenberg spins may be important in determining the energy of a defect configuration if the density of defects is

not very small. Even if we disregard this complication and other possible ones arising from spin-wave interactions and couplings between spin-wave and topological excitations, we are left with a system that corresponds to a grand canonical ensemble of positive and negative point "charges" interacting via a linear potential. The statistical mechanics of this system is difficult to work out, and no information is available at present on whether this system exhibits any "unbinding" transition at a finite temperature. An investigation (either analytic or numerical) of this question would be of considerable interest.

ACKNOWLEDGMENTS

We are grateful to A. Chakrabarti for help in the numerical computations, and to S. Chakravarty, B. I. Halperin, and B. S. Shastry for helpful discussions. The numerical work was made possible by a grant from the Minnesota Supercomputer Institute. One of us (C.D.) acknowledges support from the Alfred P. Sloan Foundation and the Indian National Science Academy.

---

*Permanent address.

[1]N. D. Mermin, Rev. Mod. Phys. **51**, 591 (1979); G. E. Volovik and V. P. Mineev, Zh. Eksp. Teor. Fiz. **72**, 2256 (1977) [Sov. Phys.—JETP **45**, 1186 (1977)].

[2]B. I. Halperin, in *Physics of Defects,* Proceedings of the Les Houches Summer Institute (North-Holland, Amsterdam, 1980).

[3]J. M. Kosterlitz and D. J. Thouless, J. Phys. C **6**, 1181 (1973).

[4]For a review, see D. R. Nelson, in *Phase Transitions and Critical Phenomena,* edited by C. Domb and J. L. Lebowitz (Academic, New York, 1983), Vol. 7.

[5]G. Kohring, R. E. Schrock, and P. Willis, Phys. Rev. Lett. **57**, 1358 (1986), and references therein.

[6]C. Dasgupta and B. I. Halperin, Phys. Rev. Lett. **47**, 1556 (1981), and references therein.

[7]J. Toner, Phys. Rev. B **26**, 462 (1982); C. Dasgupta, Phys. Rev. A **27**, 1262 (1983).

[8]R. M. J. Cotterill, in *Proceedings of the NATO Advanced Summer Institute, Geilo,* edited by T. Riste (Plenum, New York, 1980).

[9]W. Döring, J. Appl. Phys. **39**, 1006 (1968).

[10]S. Ostlund, Phys. Rev. B **24**, 485 (1981).

[11]G. S. Rushbrooke, G. A. Baker, and P. J. Wood, in *Phase Transitions and Critical Phenomena,* edited by C. Domb and M. S. Green (Academic, New York, 1974), Vol. 3.

[12]K. Binder and H. Muller-Krumbhaar, Phys. Rev. B **7**, 3297 (1973), and references therein.

[13]J. C. Le Guillou and J. Zinn-Justin, Phys. Rev. B **21**, 3976 (1980).

[14]A. M. Polyakov, Phys. Lett. B **59**, 79 (1975); E. Brezin and J. Zinn-Justin, Phys. Rev. Lett. **36**, 691 (1976); Phys. Rev. B **14**, 3110 (1976); D. R. Nelson and R. A. Pelcovits, *ibid.* **16**, 2191 (1977).

[15]R. A. Pelcovits, Ph.D. thesis, Harvard University, 1978 (unpublished).

[16]J. L. Cardy and H. W. Hamber, Phys. Rev. Lett. **65**, 499 (1980).

[17]M.-h. Lau and C. Dasgupta, Phys. Rev. B **35**, 329 (1987).

[18]S. Chakravarty, B. I. Halperin, and D. R. Nelson, Phys. Rev. Lett. **60**, 1057 (1988).

[19]A. Holz and C. de Gong, Phys. Rev. B **37**, 3751 (1988).

[20]P. B. Wiegmann, Phys. Rev. Lett. **60**, 821 (1988).

[21]A. M. Polyakov, Pis'ma Zh. Eksp. Teor. Fiz. **20**, 430 (1974) [JETP Lett. **20**, 194 (1974)]; G. 'tHooft, Nucl. Phys. B **79**, 276 (1974).

[22]M.-h. Lau and C. Dasgupta, J. Phys. A **21**, L51 (1988).

[23]J. Tobochnik and G. V. Chester, Phys. Rev. B **20**, 3761 (1979).

[24]B. Berg and M. Lüscher, Nucl. Phys. **B190**, [FS3], 412 (1981).

[25]See, e.g., *Monte Carlo Methods in Statistical Physics,* edited by K. Binder (Springer-Verlag, Berlin, 1979).

[26]M. N. Barber, in *Phase Transitions and Critical Phenomena,* edited by C. Domb and J. L. Lebowitz (Academic, New York, 1983).

[27]K. Binder, Z. Phys. B **43**, 119 (1981).

[28]R. N. Bhatt and A. P. Young, Phys. Rev. Lett. **54**, 924 (1985); A. Chakrabarti and C. Dasgupta, Phys. Rev. Lett. **56**, 1404 (1986).

[29]C. H. Papadimitriou and K. Steiglitz, *Combinatorial Optimization* (Prentice Hall, New York, 1982).

[30]The observed sample-size dependence of $\langle M \rangle$ at $K=0$ is also consistent with the form $\langle M \rangle = AN^{-a}$ with $a \simeq 0.115$. Such an N dependence would correspond to a phase with quasi-long-range order in which correlations decay algebraically with distance. Since there is no reason to expect such an unusual phase and since other thermodynamic data do not show any indication of a transition from the conventional ordered phase at low T to a new phase at high T, we prefer to interpret the results as indication of the persistence of long-range order at all temperatures.